Proteomic Profiling of the Brain of Mice with Experimental Cerebral Malaria

Ehab Moussa [1,2,4], Honglei Huang [1], Malika Ahras [3], Amar Lall [3], Marie L Thezenas[1], Roman Fischer [1], Benedikt M Kessler [1], Arnab Pain [2], Oliver Billker [3], and Climent Casals-Pascual[1]

Running title: Brain Proteome Profile of Mice with Cerebral Malaria

Affiliations:

[1] Wellcome Trust Centre for Human Genetics, Oxford, UK

[2] King Abdulla University of Science and Technology, Saudi Arabia

[3] Wellcome Trust Sanger Institute, Cambridge, UK

[4] Present Address: College of Pharmacy, Purdue University, USA

[*] Corresponding to:

Climent Casals-Pascual, MD, PhD

Wellcome Trust Centre for Human Genetics

& Centre for Cellular and Molecular Physiology

Roosevelt Drive,

Oxford, OX3 7BN, UK

ccasals@well.ox.ac.uk

Tel. 01865 287784

Fax. 01865 287787

Abstract

Cerebral malaria (CM) is a severe neurological complication of malaria infection in both adults and children. In pursuit of effective treatment of CM, clinical studies, postmortem analysis and animal models have been employed to understand the pathology and identify effective interventions. In this study, a shotgun proteomics analysis was conducted to profile the proteomic signature of the brain tissue of mice with experimental cerebral malaria (ECM) in order to further understand the underlying pathology. To identify CM-associated response, proteomic signatures of the brains of C57/Bl6N mice infected with *P. berghei* ANKA that developed neurological syndrome were compared to those of mice infected with *P. berghei* NK65 that developed equally high parasite burdens without neurological signs, and to those of non-infected mice. The results show that the CM-associated response in mice that developed neurological signs comprise mainly acute-phase reaction and coagulation cascade activation, and indicate the leakage of plasma proteins into the brain parenchyma.

Key words

Plasmodium falciparum, cerebral malaria, coagulation, acute phase reaction,.

List of abbreviations

ABC: ammonium bicarbonate

AUC: area under the curve

BBB: blood brain barrier

CID: collision-induced dissocation

CNS: central nervous system

CRP: C-reactive protein

ECM: experimental cerebral malaria

FA: formic acid

FASP: filter aided sample preparation

GAPDH: glyceraldehyde 3-phosphate dehydrogenase

HPLC: high performance liquid chromatography

IAA: iodoacetamide

IL-6: interleukin-6

PbA: Plasmodium berghei ANKA

PCA: principal components analysis

PVDF: polyvinylidene fluoride

SAA: serum amyloid A

SM: severe malaria

UA: urea

Introduction

Cerebral malaria (CM) is a severe neurological complication of *Plasmodium falciparum* infection. Children with CM usually present with a short history of fever, coma and convulsions [1]. In African children, most deaths due to CM occur within 1-2 days of admission. While the majority of children may recover consciousness in 2-3 days if treated early and appropriately, 20% of the survivors suffer neurological sequelae [1, 2].

The pathogenesis of CM has been extensively studied using animal models and postmortem analysis of patients in malaria-endemic regions. However, postmortem analysis of human brains offers only an end stage view of the pathology. Accordingly, experimental models have been used to study the brain's microvascular environment and to test new interventions. C57/Bl6 and CBA mice infected with *Plasmodium berghei* ANKA (PbA) constitute an experimental model that is widely used to study CM because it consistently reproduces neurological manifestations [3]. The neurological syndrome is typically observed 6-14 days post infection and causes mortality of up to 90%. Manifestations of the disease in mice are similar to clinical features of human CM (HCM), including signs of hemi- or paraplegia, deviation of the head, ataxia, and convulsions.

Despite these similarities, the etiology of CM in humans and ECM may differ in some important aspects. Human CM is associated with the massive obstruction of brain vasculature by sequestered infected erythrocytes [4, 5]. In the murine model, less sequestration of infected erythrocytes has been reported [6], and ECM consists primarily of an inflammatory

process characterized by the massive sequestration and infiltration of leukocytes in the brain [7]. On the other hand, modest sequestration of PbA infected red blood cells has been reported to distinguish this parasite strain from the genetically nearly identical NK65 strain, which does not cause ECM [8]. Inflammation plays an important role in CM in both systems [6, 7], as do platelet activation and coagulopathy, which contribute to organ dysfunction and vascular damage [9, 10].

Leukocytes and parasite-infected erythrocytes have been shown to adhere to intercellular adhesion molecule-1 (ICAM-1), which is up-regulated in brain endothelial cells (ECs) in both humans and mice infected with *Plasmodium* parasites [11]. In accordance, ICAM-1 knockout mice infected with PbA did not develop neurological manifestations [12]. In ECM, parasites activate monocytes either directly or indirectly through the stimulation of T-helper-1 (TH-1) cells that secrete interferon-gamma (IFN-γ). Activated monocytes then express both soluble and transmembrane tumor necrosis factor (sTNF and mTNF) that result in up-regulation of ICAM-1 on the cell surface [3]. Additionally, platelets express leukocyte function-associated antigen-1 (LFA-1) that binds to ICAM-1 on the EC surface, leading to platelet sequestration and obstruction of brain vasculature.

Another possible mechanism of CM is the permeabilization of the blood brain barrier (BBB) that occurs 2-3 days post infection in ECM and induces the activation of microglia as well as reactive changes in astrocytes [13]. These changes are followed by microglia expression of TNF, damage of astrocytes and activation of the immune system [11]. Microglial activation and astrogliosis have been observed in HCM as reflected by the up-regulation of MRP8 and MRP14 [14]. Changes in microglia and astrocytes may affect brain parenchyma and lead to adverse neurological effects that may account for the long-term neurological sequelae in the recovering patients.

The pathophysiological changes shared by ECM and HCM, the high incidence and reproducibility of the neurological syndrome in mice and the availability of genetically modified mice encourage the use of the mouse model to elucidate the pathogenesis of CM. The murine model has significantly contributed to the current understanding of the pathogenesis of CM, which has been critical to develop new therapeutic strategies and to test new interventions that cannot be directly tested in clinical trials [15].However, resistance of mice to *P. falciparum* infection and the irreversibility of the neurological syndrome limit the extrapolation of results from the murine model to human trials [16]

In an effort to understand the pathological mechanisms of the disease in mice as a model for HCM, we characterized the brain response of ECM using proteomic analysis to profile the brain proteome of C57/Bl6N mice infected with PbA that developed neurological signs compared to mice infected with *P. berghei* NK65 (Pb NK65) that did not develop neurological signs and to non-infected mice. The results show that CM-associated response in mice that developed neurological signs comprise mainly acute-phase reaction and coagulation cascade activation, and indicate the leakage of plasma proteins into the brain parenchyma.

Methods

Experimental model

Infections were carried out in the Wellcome Trust Sanger Institute, Hinxton, Cambridge, under license from the UK Home Office. Twelve wild type C57/Bl6N mice were used for this study. Four mice were infected intraperitoneally with 10^6 PbA parasitized erythrocytes, 4 mice were infected with 10^6 Pb NK65 (New York) parasitized erythrocytes, and 4 mice were injected with PBS only. To assess the neurological syndrome of murine cerebral malaria quantitatively and terminate experiments at a humane endpoint, infected mice were scored on a rapid murine coma and behavior scale (RMCBS) similar to that described by Carroll *et al*. [17]. From the morning of day 5 post infection, mice were scored twice daily for behavioral parameters including gait, balance, motor performance, posture, grip strength, touch escape, pinna reflex and toe pinch reflex. Points were awarded for each tested parameter depending on whether it was normal (2 points), mildly affected (1 point) or severely affected (0 points). ECM samples were obtained from PbA infected C57/Bl6N mice between days 6 to 7 when RMCBS score dropped to ≤10. Such mice typically had a parasitemia of 4-15% and often suffered from seizures. In preliminary experiments, hematoxylin and eosin staining of fixed brain sections showed an RMCBS score ≤10 associated with massive accumulation of leukocytes in the brain vasculature and with hemorrhages. We also observed widespread disruption of vascular integrity in the brain of such mice using intravenous injection of 2% Evans blue dye [18]. Pb NK65 infected mice were sacrificed at a time and parasitemia to match the PbA infected mice. Sham infected mice were sacrificed on day 7 post infection.

Control mice did not develop neurological symptoms and were characterized by RMCBS scores of 15 or 16 at the time their brains were obtained. As expected, mice with such high RMCBS scores did not show vascular occlusions in preliminary experiments and were characterized by an intact blood-brain-barrier, as determined by Evans blue infusion. Mice were perfused with PBS and whole brain samples were dissected and immediately snap-frozen in liquid nitrogen.

Sample processing

Brains were cut into two halves, one of which was used for proteomic profiling. Each half was minced in five volumes of cold phosphate buffered saline (PBS) with protease inhibitor cocktail (Roche) then gently centrifuged (100xg for one minute) to pellet the tissue. The pelleted tissue was homogenized in sodium dodecyl sulphate and dithiothrietol (SDS-DTT) buffer (0.175 M Tris HCL, pH 8.8, 5%SDS, 0.3 M DTT, 6 M Urea, and 2M thiourea) to which protease inhibitor cocktail (Roche) and phosphatase inhibitor cocktails 2 and 3 (Sigma) were added. Tissue homogenization was done using the Ultra-Turbax T8 homogenizer (IKA LABOR TECHNIK) at maximum speed for 30 seconds. Homogenized samples were sonicated on ice for 30 seconds to break down DNA and then spun at 500xg for 5 minutes to check homogenization efficiency. Supernatants were collected and 4 volumes of ice cold 100% acetone were added immediately, mixed by vortexing and then placed at -20 °C for one hour to precipitate proteins. Samples where then centrifuged for 15 minutes at 5000xg to collect precipitated proteins that were then washed twice with 1.5 ml of cold 80% acetone. The final pellet was resuspended in 0.5-1 ml urea buffer (6 M urea buffer, 100 mM Tris HCL, pH 7.8) and then spun for 5 minutes at 5000xg to collect soluble proteins in the supernatants and hydrophobic proteins in the pellets that were then resuspended in SDS-DTT buffer. Total protein concentrations were quantitated using fluorescence quantitation kit EZQ (Invitrogen).

Protein digestion

Pelleted hydrophobic proteins were digested using a modified filter aided sample preparation (FASP) protocol as described previously [19]. Briefly, 250 μg of cell lysates and up to 250 μl of UA buffer (8 M urea, 0.1 Tris HCL, pH 8.5) were filtered in Amicon ultra-0.5, 30 K vertical-filters (Millipore) at 14000xg for 20 minutes and followed by 2 dilution/re-concentration steps in 250 μl UA buffer at the same speed for 20 minutes each and discarding flow-thought fractions. The samples were then mixed with 100 μl iodoacetamide (IAA)

solution (0.05 M IAA in UA buffer) at 500 rpm for one minute and incubated at room temperature and then centrifuged at 14000xg for ten minutes. Filters were then washed with 250 µl UA buffer at 14000xg for 20 minutes followed by three washing steps in 250 µl ABC (0.05 M NH_4HCO_3 in water) at the same speed for 20 minutes each. Proteins were then digested overnight at 37 °C in 80 µl ABC and trypsin solution (in ABC) enough to make a trypsin to protein ratio of 1:40. Filters were then centrifuged upside down at 14000xg for one minute then washed with 100 µl 0.5 M NaCl and centrifuged upside down at 14000xg for another minute. Filters were then washed with 100 µl water and centrifuged upside up at 14000xg for ten minutes. Formic acid (FA) was added to a final concentration of 5% to stop trypsin and peptides were then purified using SEP-PACK C18 columns (Waters) and eluted with 0.6 ml buffer B (65% HPLC grade ACN and 0.1% FA) twice. Purified peptides were then vacuum dried completely in a speed-vac (Thermo) and resuspended in 100 µl of Buffer A (2% ACN, 0.1% FA).

Liquid chromatography and tandem mass-spectrometry (LC-MS/MS)

Tryptic peptides (0.5 µg) were injected into LC-MS/MS and run in technical replicates to achieve between-run and total precision. Peptide separation was carried out using a nano-UPLC system by a 75 µm-inner diameter x 25 cm C18 nanoAcquity UPLC™ column (Waters) with 2 h gradient of 2-40% solvent B (solvent A: 99.9% H2O, 0.1% FA; solvent B: 99.9% ACN, 0.1% FA). The nanoAcquity UPLC system (final flow rate, 0.25 µl/min) was coupled to the Orbitrap Velos (Thermo) mass spectrometer (MS). MS scan was performed in positive mode on the Orbitrap with mass range: 300-2000 (m/z) and mass resolution: 30000, analyzing 20 peaks of most abundant precursor ions with exclusion list of 500 and a dynamic exclusion duration of 20s. Fragmentation was done in CID mode in the iontrap at collision energy 35 V.

Proteomic Data processing

LC-MS/MS analysis were processed using label –free quantitation with Progenesis LC-MS (Nonlinear Dynamics, version 4.0). The database search was done against IPI_mouse database (Mouse, v3.56) using MASCOT [20]. All searches were conducted with the following parameters: peptide tolerance, 20 ppm; $^{13}C = 1$; fragment tolerance, 0.5 Da; number of allowed missed cleavages, 1. To normalize data, one run was selected automatically as a reference. For each feature, quantitative abundance ratio was then calculated between each run and the reference run. Only features used for proteins identification were used for normalization. Progenesis QI, the software used for label-free quantitation, automatically assigns the most suitable conditions for retention time alignment and also normalization reference. The automatic selection is based on a number of matching features and median retention time drifts. To correct for retention time drift across all runs, a reference run was selected to gauge the suitability of all other runs in the experiment. The detection of peaks across all aligned runs was performed by automatic mode and using a noise estimation algorithm to determine the signal-to-noise levels in these data.

Western blot validation of differentially expressed proteins in mice infected with PbA, and Pb NK65 as compared to control mice

Western blot analysis was performed using brain lysates from mice infected with ANKA, NK65 and controls (n=4). Twenty five milligrams of brain homogenate was lysed in SDS-DTT buffer and loaded into 4-12% SDS-PAGE gel (Bio-Rad). The proteins were transferred to PVDF membranes (Merck Millipore). Membranes were incubated with rabbit anti-mouse hemopexin (Ab90947, 1:100 diluted), albumin (Ab7793 at 1:2500 diluted). Rabbit Anti mouse GAPDH (Cell signalling, mAb #2118, 1:1000 dilute) was used as loading control (1:1000 dilute) (Sigma). Dye-800-conjugated secondary anti rabbit antibodies were applied

and visualized with an Odyssey Clx (Li-Cor).

Statistical analysis

One-way analysis of variance (ANOVA) and calculation of false discovery rate (FDR) on protein expression level were done using statistical software SPSS v19.0 (IBM). Principal component analysis (PCA) was performed using Origin Pro 9 (OriginLab). Hierarchical clustering was performed and heat maps were generated using PermutMatrix 1.9.3 [21]. Clustering was done with the following parameters, distance: Pearson centered, and aggregation: average linkage UPGMA. Significance Analysis of Microarray (SAM) was performed using Multiple Array Viewer MeV 4.8 [22].

Results

Characterization of the brain proteome of infected and non-infected C57/Bl6N mice

Neurological signs of ECM (ranging from mild ataxia to paralysis) were observed between days 6-7 of infecting C57/Bl6N mice with PbANKA, but not in PbNK65 or uninfected mice. ECM in our model was associated with strong sequestration of leukocytes in capillaries of the brain (Figure S1). The brain proteome of 12 C57/Bl6N mice was characterized using shotgun label-free quantitative proteomic analysis. Brain tissue of mice infected with PbA was compared to that of mice infected with Pb NK65 that did not develop any neurological signs, and to control non-infected mice. Collectively, 2,248 proteins were identified in both supernatants and pellets. Only proteins identified with unique peptides were considered for further analysis. Of these proteins, 521 were uniquely identified in supernatants, 488 were uniquely identified in pellets, and 1,239 proteins were identified in both. Enriched cellular components Gene Ontology (GO) terms of the genes encoding the identified proteins were obtained using EASE functional annotation tool with a Fisher-Exact P-value threshold of 0.05. Of the identified proteins, 279 plasma membrane, 273 cytoskeleton, 246 organelle membrane, 170 cytosol, 107 synapse, 112 cell junction, and 122 ribonucleoprotein complex proteins were detected (Figure 1a). Smaller groups including plasma proteins were classified together under the miscellaneous group.

PbA infected mice exhibit CM-associated response

Relative abundance of proteins across samples was quantified by the alignment of retention time spectra and comparing the AUCs of the respective peptide features. One-way ANOVA was used to produce a preliminary list of differentially expressed proteins between the three groups of mice. Adjusted P-values (Q-values) were calculated using the characteristics of P-value distribution. At FDR 1%, 170 differentially expressed proteins were identified among

the three groups of mice (Table S1). Diverse enriched cellular components GO terms were identified among the genes encoding the 170 proteins (Figure 1b). A schematic diagram of the statistical analysis employed in this study is outlined in Figure 2.

To validate the variability across the groups, a first unsupervised hierarchical clustering of all the detected proteins was done. This analysis grouped PbA infected mice together and showed an overlap between Pb NK65 infected and control non-infected mice (Figure 3a). This overlap is probably due to the large background set of non-differentially expressed proteins. Hierarchical clustering based on the preliminary set of differentially expressed proteins correctly assigned eleven mice into their biological groups. One Pb NK65 infected mouse was incorrectly clustered with control non-infected mice (Figure 3b).

ECM is associated with changes in the coagulation cascade, acute phase response and inflammation

To identify CM-associated proteomic signature and hence CM-associated host response, a strict statistical approach was applied to the data set. First, SAM was applied to identify which proteins were significantly differentially expressed in mice that developed SM (n=8) compared to non-infected control mice (n=4). A set of 345 differentially expressed proteins in mice with SM were identified with 1000 permutations at FDR 1%. SAM was then applied to this set to identify differentially expressed proteins in mice with CM compared with mice with severe non-CM. This analysis identified 59 proteins predominantly associated with CM at FDR 1% (Figure 4a and Table S2).

Principal component analysis (PCA) based on individual protein expression patterns of the 59 proteins reduced data variables into 2 components that explain 99 % of the variability among the proteins and clustered individual mice together (Figure 4b). Moreover, hierarchical clustering of the 59 proteins (Figure 5, horizontal clusters) grouped PbA infected

mice with higher confidence compared to the 170 set (Figure 2b), which confirms the CM-association of the 59 proteins. In both PCA and hierarchical clustering, PbA mice clustered together, albeit with more variability compared to the other two groups (Figures 4b and 5), whereas Pb NK65 and non-infected mice showed some overlap. Using a Fisher-Exact P-value threshold of 0.05, 14 biological process GO terms were strongly enriched in the annotation categories (Table S2). These terms fell into two main functional categories: coagulation, and acute phase response and inflammation.

CM protein coexpression patterns

To further validate proteins associated with CM and identify response patterns among them, the 59 CM-associated proteins were hierarchically clustered based on their expression profiles (Figure 5, vertical clusters). This analysis classified the proteins into 4 distinct clusters within which proteins have similar expression (co-expression) patterns across all mice (Figure 5, Table S3). Most proteins in cluster 1 exhibited a sharp fold increase between Pb NK65 and PbA compared to the fold increase between control and Pb NK65 mice. Among the proteins that had similar expression patterns in cluster 1, 5 acute phase proteins and 4 proteins of the coagulation cascade were identified. Cluster 3, however, included acute phase and coagulation cascade proteins which had different expression patterns from those found in cluster 1. The proteins in cluster 2 included the von-Willebrand factor (vWF), 6 proteins involved in ion binding, and 3 proteins involved in transcription regulation. Cluster 4 included few proteins that do not seem to be related in function.

CM-associated response contains high levels of plasma proteins in the brain

At 1% FDR, 21 plasma proteins were found to be differentially expressed across the groups and exhibited more than a 3 fold-increase in mice that developed neurological symptoms compared with mice with SM that did not develop neurological symptoms (Figure 6). Of

these, 17 were proteins that are found in high abundance in plasma of healthy C57/Bl6N mice suggesting potential “leakage” [23]. Of these, 11 proteins exhibited progressive patterns with more than 2 fold- increase in mice with SM compared with non-infected mice (Figure 6). Interestingly, most of these proteins were identified as CM-associated and grouped together in cluster 1 (Table S3).

Biochemical validation of representative proteins using western blot

The levels of hemopexin and albumin from cluster 1 (Figure 6a-b) were chosen for validation using western blotting (Figure 7). Hemopexin increased in both Pb NK65 and PbA infected brain tissues as compared to control mice and in PbA compared to Pb NK65. Albumin was significantly increased in PbA infected mice brains as compared to Pb NK65 and to control mice. The results of the Western blots of these two representative proteins agrees with protein expression measured in the proteomics study.

Discussion

In the present study, we have characterized the brain proteome of C57/Bl6N mice infected with PbA and compared it to NK65 and no infection as controls. The major finding from the brain proteome analysis suggests that changes in vascular permeability leading to plasma protein "leakage" into the brain parenchyma may play a major role in the development of ECM.

We have characterized the proteomic signatures of the brains of C57/Bl6N mice infected with PbA that developed ECM, mice infected with Pb NK65 that did not develop ECM, and control non-infected mice. The protocol was optimized to increase the brain proteome coverage to include membrane proteins of biological significance to CM pathogenesis. Following this protocol, the identified proteins covered reasonable numbers of plasma membrane, organelle membrane, and synapse proteins that were suitable to study the pathophysiology of CM in experimental models. Statistical analysis of the brain proteome data was adapted from an established approach for analyzing mice brain microarray data [24]. SAM is a statistical analysis method used for microarray data to measure the correlation between expression profiles and outcome using a non-parametric permutation-based analysis that overcomes the limitations of the equal variance and gene independence assumptions of ANOVA [25]. Using this rigorous and strict statistical analysis, we identified 59 host proteins that were significantly and differentially expressed in mice infected with PbA. These proteins were significantly correlated with ECM compared to severe non-CM infected and to non-infected mice (Table S2).

Retinal and petechial brain hemorrhages have been correlated with CM in children [26]. Moreover, petechial hemorrhage was observed in the late stages of ECM [27]. Cytokine-mediated EC activation, platelet adhesion to ECs and/or high levels of circulating EC- and

platelet-derived microparticles activate coagulation in CM [28]. In line with previously reported pathophysiological changes, the proteins associated with ECM identified in the present study include 4 members of the coagulation cascade that were strongly enriched: fibrinogen (alpha and gamma chains), kininogen-1, plasminogen, and vWF. The up-regulation of vWF is plausible indicative of platelet adhesion in the brain microvasculature of mice with ECM, and is consistent with observations in human CM in which the role of vWF has been well-characterized [29]. Furthermore, higher levels of fibrinogen, kininogen-1 and plasminogen may indicate an ongoing state of hyper-coagulation in the brain microvasculature.

In general, cytokines associated with inflammation stimulate the production of acute-phase proteins [30]. In children, CM has been associated with high levels of IL-6, IL-10, and TNF-α in the plasma [1]. In adults, two major acute-phase proteins, SAA-1 and CRP, were found to be associated with severity of SM [31]. Similarly to humans, the interplay of inflammation and coagulation is of particular interest in mouse models [32]. Here, 11 acute-phase proteins were enriched among the significantly differentially expressed proteins, including alpha-2-HS-glycoprotein, complement factor D (adipsin), fibrinogen (alpha and gamma chain), kininogen 1, orosomucoid 1, orosomucoid 2, plasminogen, serum amyloid A 1, hemopexin, and transferrin. Together with the up-regulation of the coagulation cascade proteins, the up-regulation of acute-phase proteins supports the cross talk of inflammation and coagulation in the pathogenesis of ECM.

To identify co-expression patterns of CM-associated proteins, we used hierarchical clustering algorithms to model the expression pattern of these proteins across all mice. This analysis grouped CM-associated proteins into 4 clusters. Among the proteins that have similar expression patterns in cluster 1 are 5 acute phase proteins: Alpha-2-HS-glycoprotein,

Alpha-1-acid glycoprotein 1, serotransferrin, hemopexin, fibrinogen alpha and kininogen-1, and 4 members of the coagulation cascade: alpha-1-antitrypsin 1-4, alpha-1-antitrypsin 1-3, fibrinogen alpha and kininogen 1. This observation indicates a possible orchestrated effect of these proteins in the pathology, possibly capturing downstream events from the original injury cascade triggered by the parasite infection. Similarly, acute phase proteins and coagulation cascade proteins were identified in cluster 3 but with a less dramatic increase in PbA compared to Pb NK65.

Interestingly, 15 out of the 59 CM-associated proteins are classical plasma proteins. We speculate that the observation of significantly high levels of these proteins is due to a "leak effect" in which plasma proteins in the brain vasculature leaked into the brain tissue. This effect implies endothelial damage and breakage of the BBB probably due to leukocyte accumulation and local cytokine release, which causes dysregulation of transport across the barrier cells. This is in accordance with the results by Brown et al. that demonstrated the leakage of plasma proteins through the BBB of Vietnamese adults [33] and Malawian children [34]. In the study in adults, immunohistochemistry on post-mortem brains demonstrated the leakage of the plasma protein fibrinogen into the perivascular space and its uptake by astrocytes end-feet [33]. In both adults and children, perivascular macrophages expressed sialoadhesin, which is only expressed in the CNS upon stimulation by plasma proteins [33, 34]. BBB permeabilization is probably the consequence of the advance stage of disease progression in this model of severe malaria. These findings have been reported previously [35, 36]

Conclusions

In summary, quantitative proteomic analysis of the brain tissue of mice infected with PbA, Pb NK65 or non-infected mice shows an enrichment of coagulation cascade and acute-phase proteins in the brains of mice that developed neurological signs. Collectively, the results highlight the role of sequestration, inflammation and coagulation in the pathophysiology of ECM. Moreover, the higher levels of plasma proteins detected in the brains of mice with ECM suggest a 'leak effect' possibly due to brain endothelial damage by sequestered parasites.

Acknowledgements

We wish to acknowledge Stanley Barkhuysen for technical assistance. The *P. berghei* NK65 (New York) line was generously provided by Robert Menard, Institut Pasteur, Paris.

Figure legends

Figure 1. Cellular component Gene Ontology terms of the brain proteome. (a) Total 2,248 identified proteins. (b) 170 differentially expressed proteins identified using One-way ANOVA.

Figure 2. Schematic diagram of the statistical analysis workflow. The right arm describes the SAM approach used to analyze the data to identify CM-associated proteins. The left arm describes traditional statistical analysis using One-way ANOVA followed by multiple t-tests to identify deferentially expressed proteins. A large subset of the CM-associated proteins identified by SAM were also in the 170 proteins set identified using ANOVA.

Figure 3. Proteomic profiles in non-infected, SM, or ECM mice. Dendrograms of individual mice (vertical) represent overall similarities in proteomic profiles. Each row represents an individual protein. Normalized protein quantitation values are represented according to the color scale at the bottom. (a) Hierarchical clustering of 12 brain samples using quantitation values of all detected proteins. (b) Hierarchical clustering of the 12 brain samples using quantitation values of 170 significant differentially expressed proteins across the three groups. Letters A, N and C represent PbANKA, PbNK65 and control mice, respectively.

Figure 4. CM-associated proteins. (a) SAM plot. The solid line is the "expected=observed" scores line, and the dashed lines represent the confidence limits thereof. The more the observed score of a given protein deviates from the "observed=expected" line, the more likely it is to be significantly differentially expressed. The value of any protein in the positive or negative direction whose observed score exceeds the expected one by at least delta (the test statistic analogous to t) is considered significant. (b) Principal component analysis (PCA) of the CM-associated proteins. PCA of 12 brain samples was carried out using quantitation values of the CM-associated proteins plotted in two components rotational space explaining

99.9% of the variability in the data. PbANKA (Closed red triangles), PbNK65 (Closed orange diamonds), and control mice (Open black circles).

Figure 5. Co-expression patterns of the CM-associated proteins. Hierarchical clustering of the brain samples using quantitation values of CM-associated proteins. Dendrograms of individual mice (vertical) and proteins (horizontal) represent overall similarities in proteomic profiles. Each row represents an individual protein. Normalized protein quantitation values are represented according to the color scale at the bottom.

Figure 6. Plasma proteins profiles. Quantitation values of 21 plasma proteins that are differentially expressed in PbANKA mice compared to PbNK65 and control mice. Bars represent mean ± SD (n=4).

Figure 7. Western blot validation of hemopexin and albumin in mice brain tissues. (a) Protein expression level of hemopexin and albumin were measured by western blot using mice brain tissues infected with PbA (n=4), Pb NK65 (n=4) or non-infected control mice (n=4), GAPDH was measured and used as a normalization baseline. (b) Hemopexin expression level was quantified and plotted, there was an increased expression of hemopexin in both Pb NK65 and PbA infected mice brain tissue as compared to control mice. (c) Albumin expression level was quantified and plotted, increased expression of albumin in PbA infected mice brain tissue as compared to Pb NK65 and control mice brain tissues were detected. Data is presented as mean ± SEM. * p-value <0.05.

Figure 1.

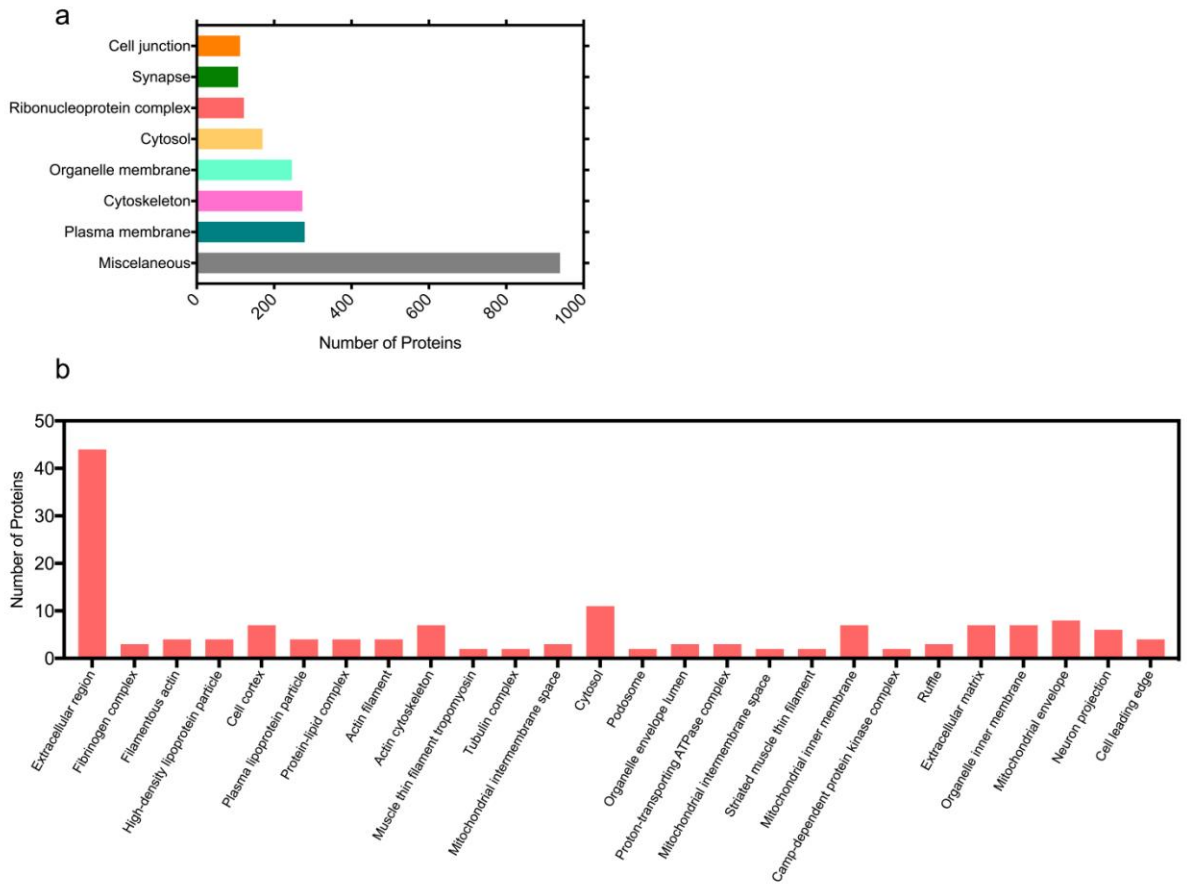
a
Cell junction
Synapse
Ribonucleoprotein complex
Cytosol
Organelle membrane
Cytoskeleton
Plasma membrane
Miscelaneous
0
200
400
600
800
1000
Number of Proteins
b
Number of Proteins
50
40
30
20
10
0
Extracellular region
Fibrinogen complex
Filamentous actin
High-density lipoprotein particle
Cell cortex
Plasma lipoprotein particle
Protein-lipid complex
Actin filament
Actin cytoskeleton
Muscle thin filament tropomyosin
Tubulin complex
Mitochondrial intermembrane space
Cytosol
Podosome
Organelle envelope lumen
Proton-transporting ATPase complex
Mitochondrial intermembrane space
Striated muscle thin filament
Mitochondrial inner membrane
Camp-dependent protein kinase complex
Ruffle
Extracellular matrix
Organelle inner membrane
Mitochondrial envelope
Neuron projection
Cell leading edge

Figure 2.

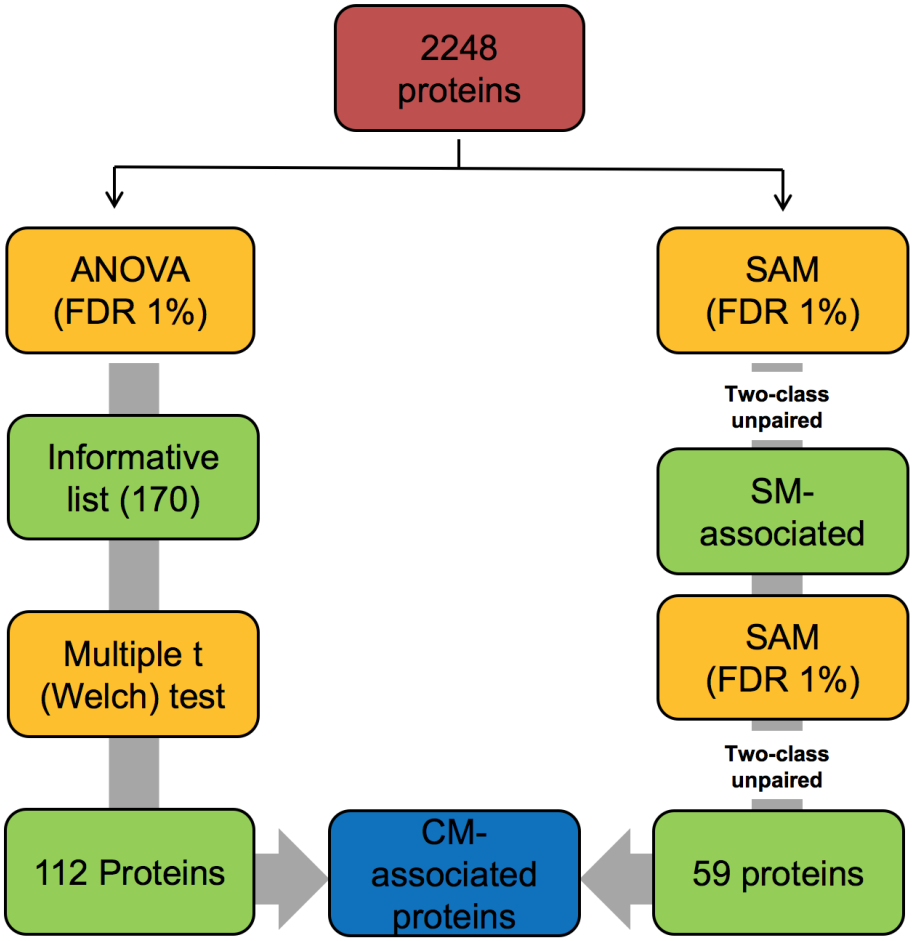
2248 proteins
ANOVA (FDR 1%)
SAM (FDR 1%)
Two-class unpaired
Informative list (170)
SM-associated
Multiple t (Welch) test
SAM (FDR 1%)
Two-class unpaired
112 Proteins
CM-associated proteins
59 proteins

Figure 3.

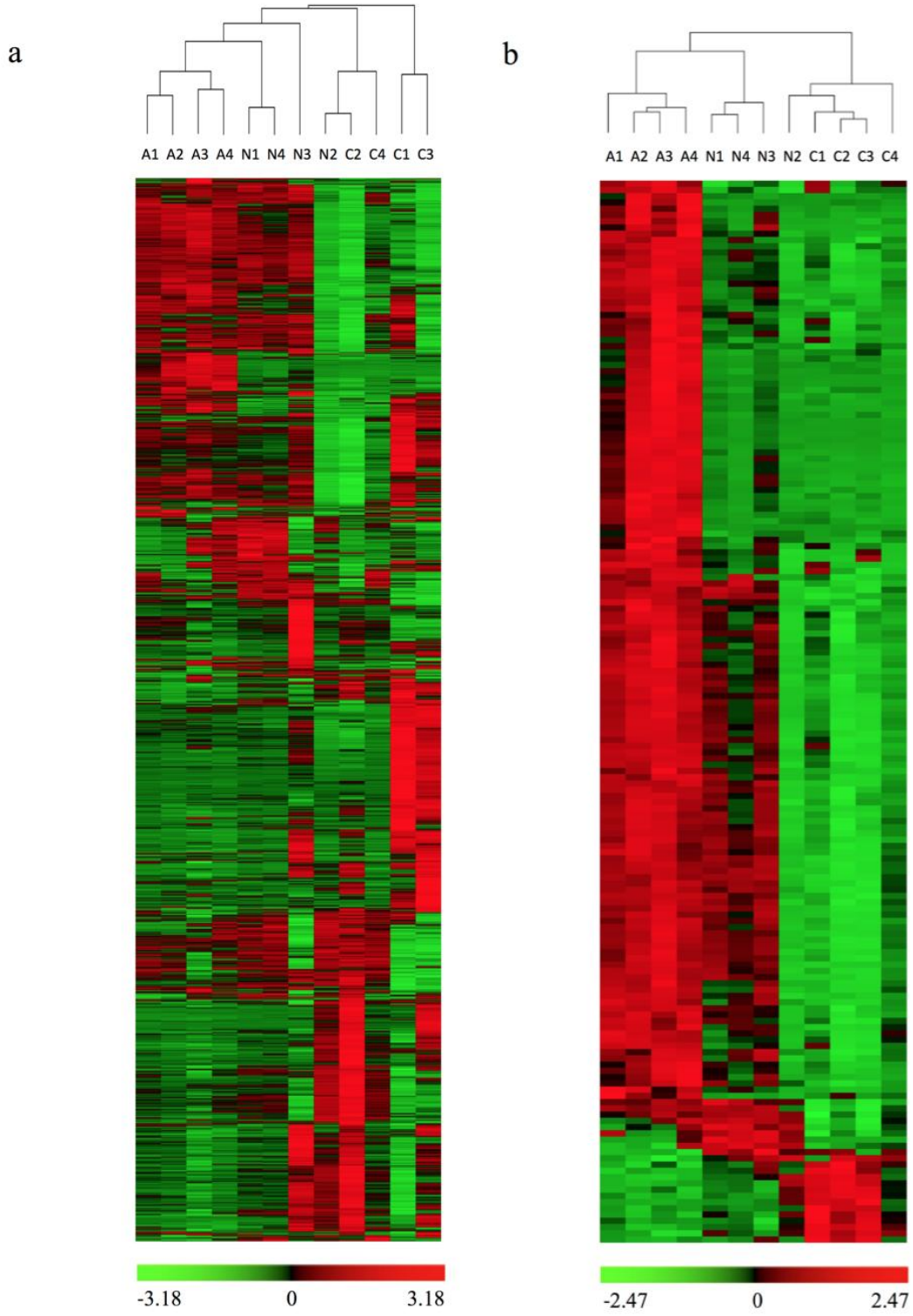
a
A1 A2 A3 A4 N1 N4 N3 N2 C2 C4 C1 C3
-3.18
0
3.18
b
A1 A2 A3 A4 N1 N4 N3 N2 C1 C2 C3 C4
-2.47
0
2.47

Figure 4.

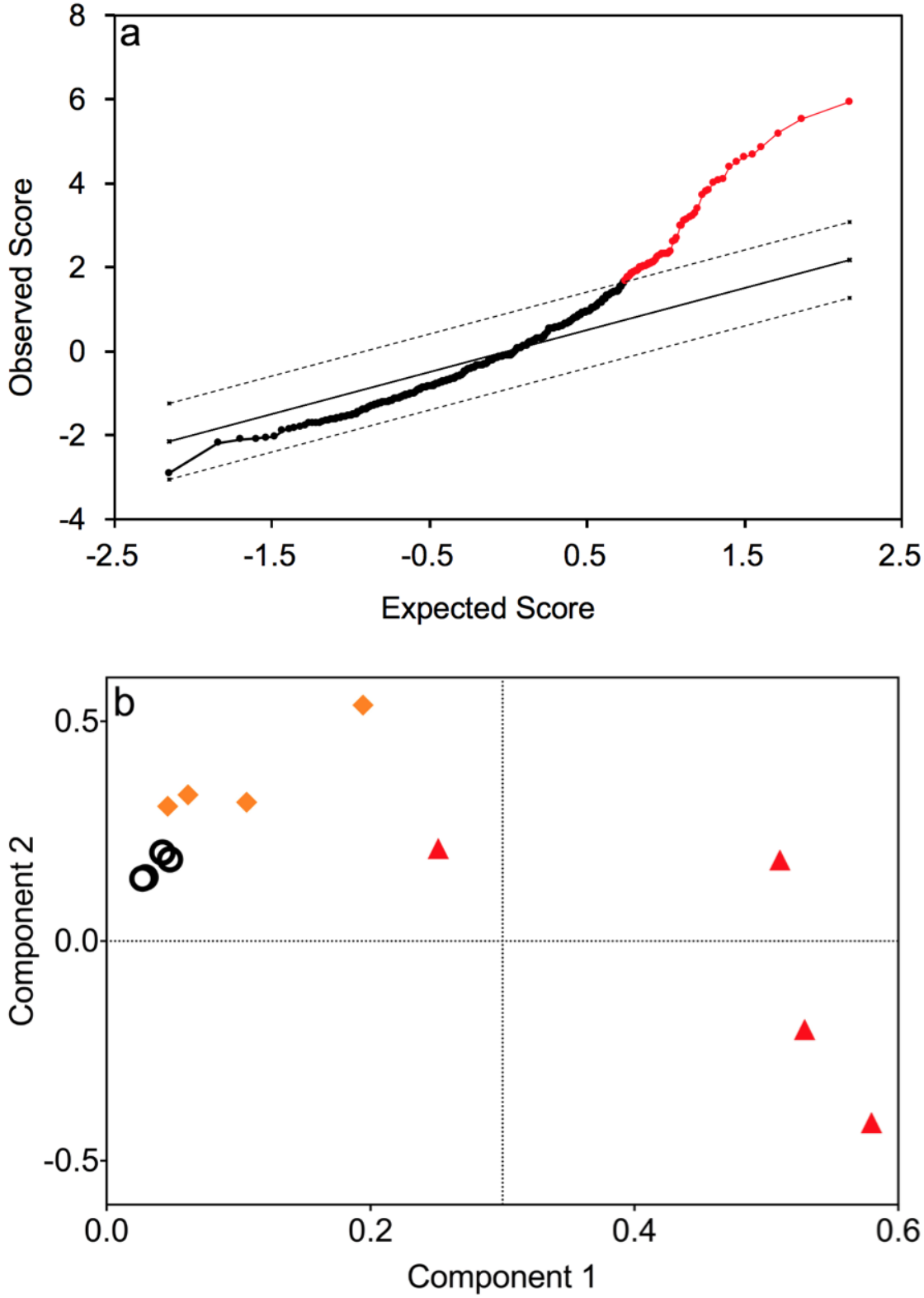
a
Observed Score
Expected Score
8
6
4
2
0
-2
-4
-2.5
-1.5
-0.5
0.5
1.5
2.5
b
Component 2
Component 1
0.5
0.0
-0.5
0.0
0.2
0.4
0.6

Figure 5.

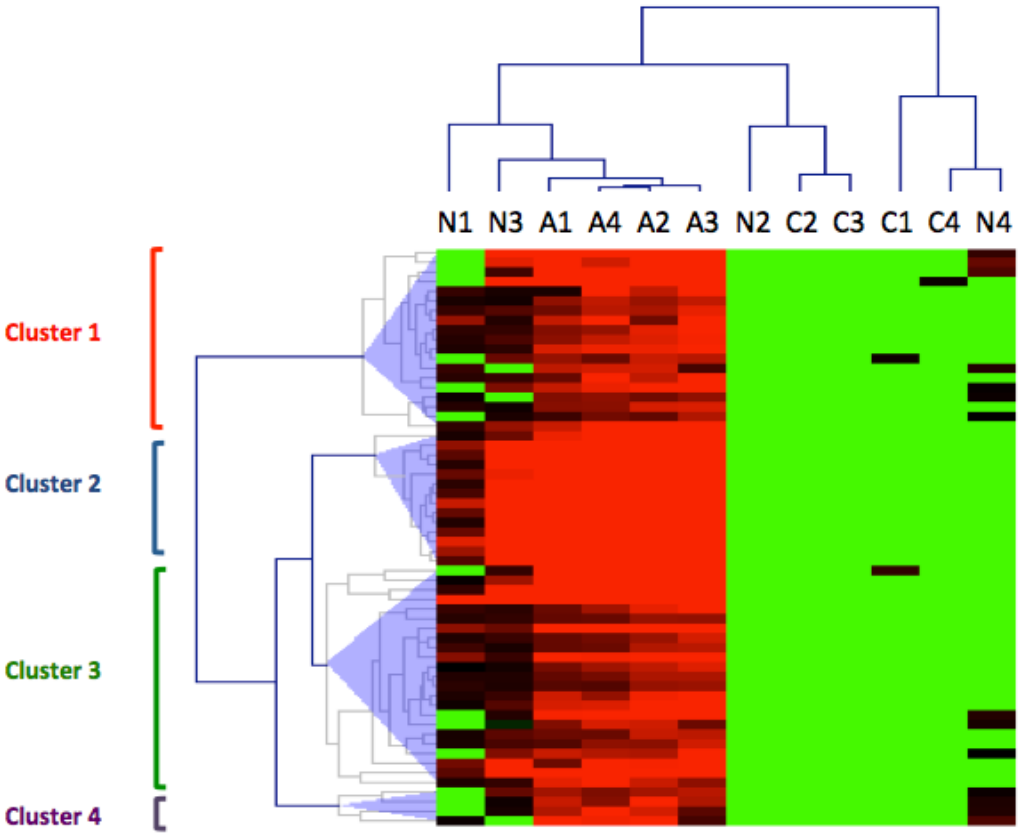
N1
N3
A1
A4
A2
A3
N2
C2
C3
C1
C4
N4
Cluster 1
Cluster 2
Cluster 3
Cluster 4

Figure 6.

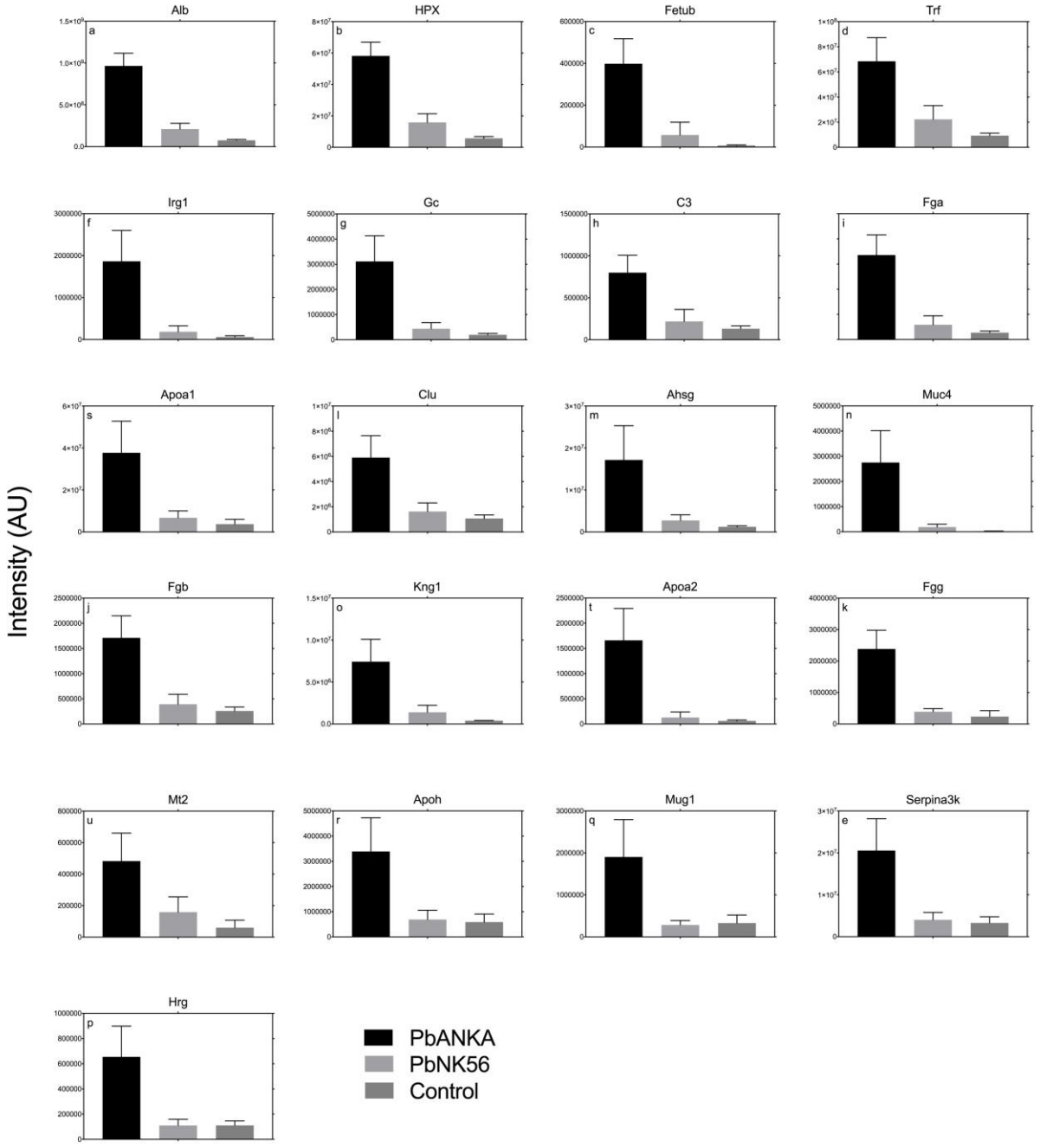
Alb
HPX
Fetub
Trf
Irg1
Gc
C3
Fga
Apoa1
Clu
Ahsg
Muc4
Fgb
Kng1
Apoa2
Fgg
Mt2
Apoh
Mug1
Serpina3k
Hrg
Intensity (AU)
PbANKA
PbNK56
Control

Figure 7.

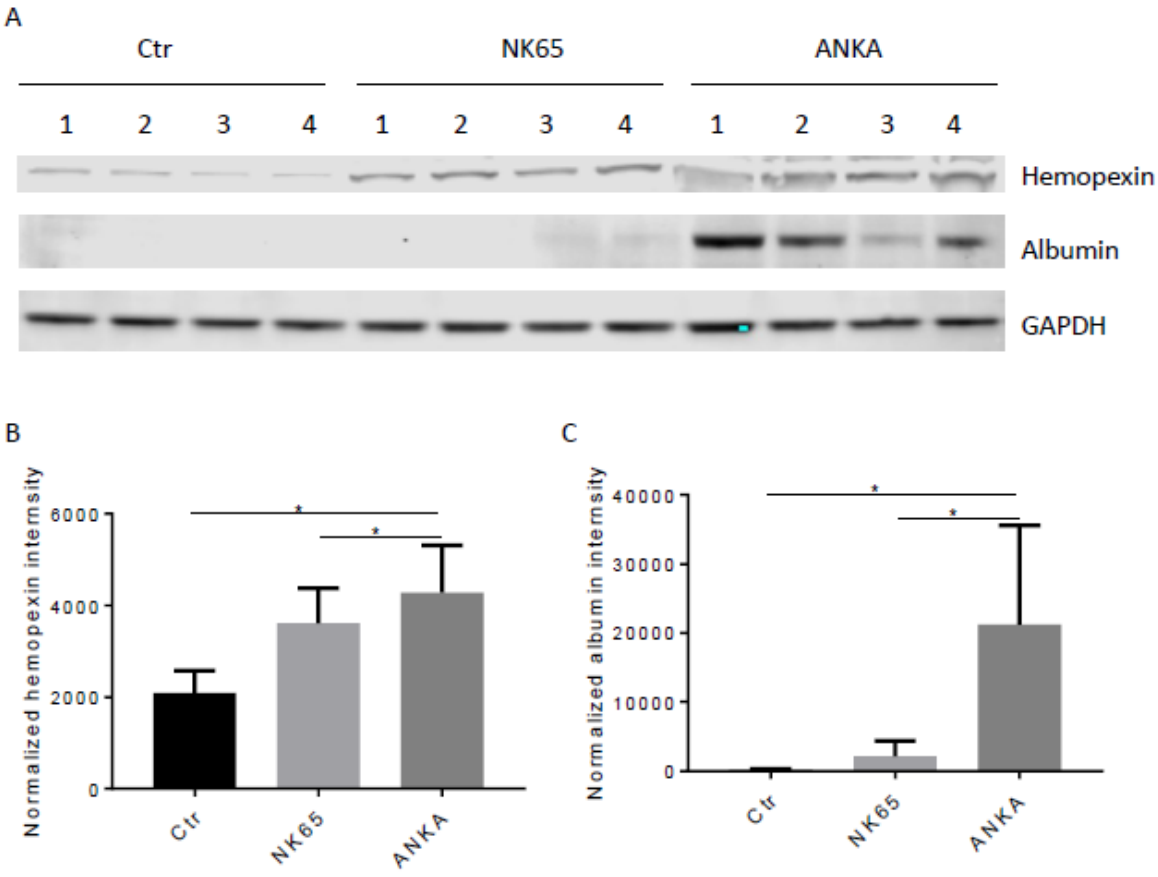
A
Ctr
NK65
ANKA
1 2 3 4 1 2 3 4 1 2 3 4
Hemopexin
Albumin
GAPDH
B
Normalized hemopexin intensity
6000
4000
2000
0
*
*
Ctr
NK65
ANKA
C
Normalized albumin intensity
40000
30000
20000
10000
0
*
*
Ctr
NK65
ANKA

References

[1] R. Idro, N.E. Jenkins, C.R. Newton, Pathogenesis, clinical features, and neurological outcome of cerebral malaria, Lancet neurology 4(12) (2005) 827-40.
[2] J. Farrar, C. Newton, Neurological aspects of tropical disease, Journal of neurology, neurosurgery, and psychiatry 68(2) (2000) 135-6.
[3] J. Lou, R. Lucas, G.E. Grau, Pathogenesis of cerebral malaria: recent experimental data and possible applications for humans, Clinical microbiology reviews 14(4) (2001) 810-20, table of contents.
[4] A.M. Dondorp, C. Ince, P. Charunwatthana, J. Hanson, A. van Kuijen, M.A. Faiz, M.R. Rahman, M. Hasan, E. Bin Yunus, A. Ghose, R. Ruangveerayut, D. Limmathurotsakul, K. Mathura, N.J. White, N.P. Day, Direct in vivo assessment of microcirculatory dysfunction in severe falciparum malaria, J Infect Dis 197(1) (2008) 79-84.
[5] E. Pongponratn, G.D. Turner, N.P. Day, N.H. Phu, J.A. Simpson, K. Stepniewska, N.T. Mai, P. Viriyavejakul, S. Looareesuwan, T.T. Hien, D.J. Ferguson, N.J. White, An ultrastructural study of the brain in fatal Plasmodium falciparum malaria, Am J Trop Med Hyg 69(4) (2003) 345-59.
[6] J. Hearn, N. Rayment, D.N. Landon, D.R. Katz, J.B. de Souza, Immunopathology of cerebral malaria: morphological evidence of parasite sequestration in murine brain microvasculature, Infection and immunity 68(9) (2000) 5364-76.
[7] D.S. Hansen, Inflammatory responses associated with the induction of cerebral malaria: lessons from experimental murine models, PLoS Pathog 8(12) (2012) e1003045.
[8] T.N. Shaw, P.J. Stewart-Hutchinson, P. Strangward, D.B. Dandamudi, J.A. Coles, A. Villegas-Mendez, J. Gallego-Delgado, N. van Rooijen, E. Zindy, A. Rodriguez, J.M. Brewer, K.N. Couper, M.L. Dustin, Perivascular Arrest of CD8+ T Cells Is a Signature of Experimental Cerebral Malaria, PLoS Pathog 11(11) (2015) e1005210.
[9] D. Cox, S. McConkey, The role of platelets in the pathogenesis of cerebral malaria, Cell Mol Life Sci 67(4) (2010) 557-68.
[10] I.M. Francischetti, Does activation of the blood coagulation cascade have a role in malaria pathogenesis?, Trends Parasitol 24(6) (2008) 258-63.
[11] N.H. Hunt, G.E. Grau, Cytokines: accelerators and brakes in the pathogenesis of cerebral malaria, Trends in immunology 24(9) (2003) 491-9.
[12] N. Favre, C. Da Laperousaz, B. Ryffel, N.A. Weiss, B.A. Imhof, W. Rudin, R. Lucas, P.F. Piguet, Role of ICAM-1 (CD54) in the development of murine cerebral malaria, Microbes and infection / Institut Pasteur 1(12) (1999) 961-8.
[13] I.M. Medana, T. Chan-Ling, N.H. Hunt, Redistribution and degeneration of retinal astrocytes in experimental murine cerebral malaria: relationship to disruption of the blood-retinal barrier, Glia 16(1) (1996) 51-64.
[14] H.J. Schluesener, P.G. Kremsner, R. Meyermann, Widespread expression of MRP8 and MRP14 in human cerebral malaria by microglial cells, Acta neuropathologica 96(6) (1998) 575-80.
[15] N.H. Hunt, G.E. Grau, C. Engwerda, S.R. Barnum, H. van der Heyde, D.S. Hansen, L. Schofield, J. Golenser, Murine cerebral malaria: the whole story, Trends in parasitology 26(6) (2010) 272-4.
[16] N.J. White, G.D. Turner, I.M. Medana, A.M. Dondorp, N.P. Day, The murine cerebral malaria phenomenon, Trends in parasitology 26(1) (2010) 11-5.

[17] R.W. Carroll, M.S. Wainwright, K.Y. Kim, T. Kidambi, N.D. Gomez, T. Taylor, K. Haldar, A rapid murine coma and behavior scale for quantitative assessment of murine cerebral malaria, Plos One 5(10) (2010).
[18] M. Wiranowska, T.C. Wilson, K.S. Bencze, L.D. Prockop, A mouse model for the study of blood-brain barrier permeability, J Neurosci Methods 26(2) (1988) 105-9.
[19] J.R. Wisniewski, A. Zougman, N. Nagaraj, M. Mann, Universal sample preparation method for proteome analysis, Nature methods 6(5) (2009) 359-62.
[20] D.N. Perkins, D.J. Pappin, D.M. Creasy, J.S. Cottrell, Probability-based protein identification by searching sequence databases using mass spectrometry data, Electrophoresis 20(18) (1999) 3551-67.
[21] G. Caraux, S. Pinloche, PermutMatrix: a graphical environment to arrange gene expression profiles in optimal linear order, Bioinformatics 21(7) (2005) 1280-1.
[22] A.I. Saeed, V. Sharov, J. White, J. Li, W. Liang, N. Bhagabati, J. Braisted, M. Klapa, T. Currier, M. Thiagarajan, A. Sturn, M. Snuffin, A. Rezantsev, D. Popov, A. Ryltsov, E. Kostukovich, I. Borisovsky, Z. Liu, A. Vinsavich, V. Trush, J. Quackenbush, TM4: a free, open-source system for microarray data management and analysis, BioTechniques 34(2) (2003) 374-8.
[23] K.K. Lai, D. Kolippakkam, L. Beretta, Comprehensive and quantitative proteome profiling of the mouse liver and plasma, Hepatology 47(3) (2008) 1043-51.
[24] N.F. Delahaye, N. Coltel, D. Puthier, L. Flori, R. Houlgatte, F.A. Iraqi, C. Nguyen, G.E. Grau, P. Rihet, Gene-expression profiling discriminates between cerebral malaria (CM)-susceptible mice and CM-resistant mice, The Journal of infectious diseases 193(2) (2006) 312-21.
[25] V.G. Tusher, R. Tibshirani, G. Chu, Significance analysis of microarrays applied to the ionizing radiation response, Proceedings of the National Academy of Sciences of the United States of America 98(9) (2001) 5116-21.
[26] V.A. White, S. Lewallen, N. Beare, K. Kayira, R.A. Carr, T.E. Taylor, Correlation of retinal haemorrhages with brain haemorrhages in children dying of cerebral malaria in Malawi, Transactions of the Royal Society of Tropical Medicine and Hygiene 95(6) (2001) 618-21.
[27] T. Chang-Ling, A.L. Neill, N.H. Hunt, Early microvascular changes in murine cerebral malaria detected in retinal wholemounts, The American journal of pathology 140(5) (1992) 1121-30.
[28] C.A. Moxon, R.S. Heyderman, S.C. Wassmer, Dysregulation of coagulation in cerebral malaria, Molecular and biochemical parasitology 166(2) (2009) 99-108.
[29] D. Larkin, B. de Laat, P.V. Jenkins, J. Bunn, A.G. Craig, V. Terraube, R.J. Preston, C. Donkor, G.E. Grau, J.A. van Mourik, J.S. O'Donnell, Severe Plasmodium falciparum malaria is associated with circulating ultra-large von Willebrand multimers and ADAMTS13 inhibition, PLoS pathogens 5(3) (2009) e1000349.
[30] C. Gabay, I. Kushner, Acute-phase proteins and other systemic responses to inflammation, The New England journal of medicine 340(6) (1999) 448-54.
[31] S.H. Gillespie, C. Dow, J.G. Raynes, R.H. Behrens, P.L. Chiodini, K.P. McAdam, Measurement of acute phase proteins for assessing severity of Plasmodium falciparum malaria, Journal of clinical pathology 44(3) (1991) 228-31.
[32] M. Levi, T. van der Poll, H.R. Buller, Bidirectional relation between inflammation and coagulation, Circulation 109(22) (2004) 2698-704.
[33] H. Brown, T.T. Hien, N. Day, N.T. Mai, L.V. Chuong, T.T. Chau, P.P. Loc, N.H. Phu, D. Bethell, J. Farrar, K. Gatter, N. White, G. Turner, Evidence of blood-brain barrier

dysfunction in human cerebral malaria, Neuropathol Appl Neurobiol 25(4) (1999) 331-40.
[34] H. Brown, S. Rogerson, T. Taylor, M. Tembo, J. Mwenechanya, M. Molyneux, G. Turner, Blood-brain barrier function in cerebral malaria in Malawian children, Am J Trop Med Hyg 64(3-4) (2001) 207-13.
[35] M. Linares, P. Marin-Garcia, S. Perez-Benavente, J. Sanchez-Nogueiro, A. Puyet, J.M. Bautista, A. Diez, Brain-derived neurotrophic factor and the course of experimental cerebral malaria, Brain Res 1490 (2013) 210-24.
[36] H. Ishida, T. Imai, K. Suzue, M. Hirai, T. Taniguchi, A. Yoshimura, Y. Iwakura, H. Okada, T. Suzuki, C. Shimokawa, H. Hisaeda, IL-23 protection against Plasmodium berghei infection in mice is partially dependent on IL-17 from macrophages, Eur J Immunol 43(10) (2013) 2696-706.